Desalination and Water Treatment
www.deswater.com

doi: 10.5004/dwt.2019.24446

164 (2019) 240–248
October

CBG-HCl as a green corrosion inhibitor for low carbon steel in 0.5 M H_2SO_4 with and without 0.1 M NaCl

Abdualah Elhebshi[a], Ahmed El Nemr[b,*], Mohamed S. El-Deab[c], Ibrahim Ashour[a,d]

[a]*Chemical Engineering Department, Faculty of Engineering, Elminia University, Elminia, Egypt, email: hebshi71@gmail.com (A. Elhebshi)*
[b]*Environmental Division, National Institute of Oceanography and Fisheries, Kayet Bey, El-Anfoushy, Alexandria, Egypt, email: ahmedmoustafaelnemr@yahoo.com, ahmed.m.elnemr@gmail.com (A. El Nemr)*
[c]*Department of Chemistry, Faculty of Science, Cairo University, Cairo, Egypt, email: msaada68@yahoo.com (M.S. El-Deab)*
[d]*Zewail City, University of Science and Technology, 6th October City, Giza, Egypt, email: ibrahim.ashour@gmail.com (I. Ashour)*

Received 19 December 2018; Accepted 20 May 2019

ABSTRACT

This research studies the inhibition efficiency (IE) of chitosan biguanidine hydrochloride (CBG-HCl), as novel environmentally - friendly organic inhibitor, contrary to the corrosion of low carbon steel (LCS) in 0.5 M sulphuric acid whether the synergistic effect of 0.1 M NaCl exists or not. Results obtained from both electrochemical impedance spectroscopy (EIS) and electrochemical polarization measurements indicated a significant increase in the corrosion protection of the low carbon steel in the presence of CBG-HCl and 0.1 M NaCl as opposed to the presence of CBG-HCl alone. The formation of a protective film by the adsorbed inhibitor blend obstructs the surface area of the LCS rod hindering corrosive gradients to react with the metal surface. The research showed that an IE of 80% was reached when 100 ppm of CBG-HCI was added along with 0.1 M NaCl whereas it only reached 66% in the absence of 0.1 M NaCl. A maximum IE of 92.67% was reported for 100 ppm CBG-HCl and 0.1 M NaCl after six hours of immersion. Furthermore, potentiodynamic experiments indicate that a CBG-HCl and 0.1 M NaCl blend acts as a mixed-type inhibitor for the corrosion of low carbon steel. Inhibition efficiency of CBG-HCl/0.1 M NaCl blend remains noticeably high with long periods of immersion indicating its good stability in the applied acidic medium.

Keywords: Chitosan biguanidine hydrochloride; Low carbon steel; EIS; Green corrosion inhibitor; Synergistic effect

1. Introduction

Carbon steel (CS) is the most applicable material in the construction of oil industry equipment, such as downhole tubules, flow lines, and transmission pipelines [1–5]. On the other hand, CS has low corrosion resistance in the corrosive environments that are related to oil industries [6]. Using corrosion inhibitors is one of the most common ways of controlling corrosion rate in acidic solutions in oil processes, such as in pickling processes, and in industrial acid cleaning. Oil and gas pipelines usually get subjected to acid cleaning for removal of rust [7–11]. The mechanism of inhibitors mostly depends on the modification of metal surfaces by the adsorption of inhibitor molecules and subsequently the formation of a protective layer. Quantum chemistry has been used in the study of protection mechanism and in the prediction of inhibition efficiency of organic compounds [12–15]. Many of the applied corrosion inhibitors are natural products that contain heteroatoms such as nitrogen, sulfur, phosphorus, and oxygen atoms which enhance adsorption of these compounds [6]. These organic compounds are used as eco-friendly corrosion inhibitors [16]. Many of these products are extracted from different parts of plants like root, seeds, leaves, stem, bark, flower, and fruits [17–21]. Literature has shown that plant leaves such as *margosa leaves*, *murraya koenigii* leaves, *ervatamia coronaria* leaves, herb leaves,

*Corresponding author.

bauhinia purpurea leaves, and olive leaves inhibit the corrosion of metals in acidic media [22–26].

Umoren et al. [27] investigated the efficiency of chitosan (a product of naturally occurring polymer chitin) as a corrosion inhibitor for mild steel in 0.1 M HCl by gravimetric, potentiodynamic polarization, electrochemical impedance spectroscopy measurements, scanning electron microscopy, and UV–visible analysis. The polymer was found to inhibit corrosion even at a very low concentration. Inhibition efficiency increases with a rise in temperature up to 96% at 60°C and then drops to 93% at 70°C, while it slightly increases with an increase in chitosan concentration. Polarization curves indicate that chitosan functions as a mixed inhibitor. Jmiai et al. [28] also investigated chitosan as a copper corrosion inhibitor in molar hydrochloric medium and the inhibition efficiency reached a maximum of 87%. Solomon et al. [29] studied the inhibiting ability of chitosan alone and in combination with KI for St37 steel in 15% H_2SO_4 solution using different electrochemical techniques and weight loss. The effect of immersion time on inhibition efficiency was examined for 15 h and the influence of temperature studied over the temperature range of 25–60°C. Results obtained from all the applied methods portray chitosan as a moderate inhibitor for St37 steel in the studied acid environment. Addition of KI was found to remarkably enhance the inhibition efficiency of the polymer above 92%. Fekry et al. [30] synthesized acetyl thiourea chitosan polymer (ATUCS) and evaluated it as corrosion inhibitor for mild steel in naturally aerated 0.5 M H_2SO_4 and has shown inhibition efficiency reaches 94.5%. Liu et al. [31] investigated inhibition of carbon steel corrosion in 0.5 M hydrochloric acid solutions by β-cyclodextrin modified natural chitosan and the results indicated that the inhibition efficiency increased with the inhibitor concentration with a maximum achievable inhibition efficiency of 96.02%.

The global concern on health hazards and environmental pollution caused by various categories of inhibitors has directed the research toward the development of green corrosion inhibitor molecules that are cheap, effective, and have low or zero negative environmental impact [7–11]. In this regard, the goal of this present research is to investigate the possibility of using chitosan biguanidine hydrochloride (CBG-HCl), which is a natural polymer derivative, as a green corrosion inhibitor for low carbon steel in acidic medium in addition to determining the efficiency and mechanism of its corrosion inhibition.

2. Materials and experiments

2.1. Solutions and chemicals

Sulfuric acid (98%) and Sodium chloride was purchased from Fluka and were used without further purification. The Corrosive solution (electrolyte) 0.5 M H_2SO_4, was prepared by diluting concentrated sulfuric acid (98%) to a required concentration using deionized water. In addition, 0.1 M of NaCl salt was added to the electrolyte as synergistic.

2.2. CBG-HCl preparation

Chitosan biguanidine hydrochloride (CBG-HCl) (Fig. 1), as a modified natural polymer, was obtained according to some modification based on literature works [32–34]. Five grams of chitosan were dissolved in 250 mL of 1 N HCl under stirring condition for 1 h at 80°C; then 2.86 g of cyanoguanidine in 50 mL H_2O, with a molar ratio of 1:1 of chitosan, was added to chitosan solution. The reaction mixture was stirred at 100°C for 5 h; then the reaction mixture was cooled to room temperature and excess ethanol was added for precipitation. The white precipitate was collected by filtration, washed with 70% ethanol and dried in a vacuum oven at 50°C to produce 8.95 g (90.59% yield). The structure was confirmed by comparing FTIR (Vertex 70 connected with Platinum ATR unit, Bruker, Germany) with that published in literature (Fig. 2).

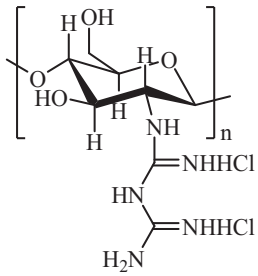

Fig. 1. Chemical structure of CBG-HCl.

2.3. Electrochemical/alloy, corrosion cell and equipment

A rod of low carbon steel alloys with the following composition (wt %): 0.068 C, 0.249 Si, 0.662 Mn, 0.015 P, 0.022 S, 0.027 Ni, 0.031 Cu, 0.122 N, 98.62 Fe and traces of other elements have been used as the working electrode. The low carbon steel rod was sealed by Teflon coat and epoxy resin leaving a two dimensional exposed surface area of 0.64 cm^2. A graphite cylindrical rod (1 cm diameter × 15 cm length tall) and a saturated calomel electrode (SCE) were used as the counter and the reference electrodes, respectively.

A conventional three-electrode glass cell was used to perform electrochemical measurements using a Gamry Potentiostat/Galvanostat (model Series-G 300) controlled with Gamry Fram work version 6.12, DC105 and EIS300 software. The impedance measurements were performed at the frequency range of 100 kHz–0.1 Hz with a peak-to-peak amplitude of 10 mV using a.c. signals under the open circuit potential (OCP) conditions of low carbon steel rod. The obtained impedance spectra were analyzed using equivalent circuit software. Scanning electron microscopy (FEI-SEM QUANTA 250) was applied to evaluate the sample surface corrosion.

2.4. Methodology of corrosion inhibitor test

Before each test, the electrode was polished on wet SiC papers, of successively finer grades. Then, washed with distilled water, degreased in ultrasonic-bath with ethanol and finally dried and immersed in the corrosive medium. The medium was 0.5 M sulphuric acid, consisting of different concentrations of CBG-HCl (25, 50, 70 and 100 ppm) during the inclusion and the exclusion of 0.1 M

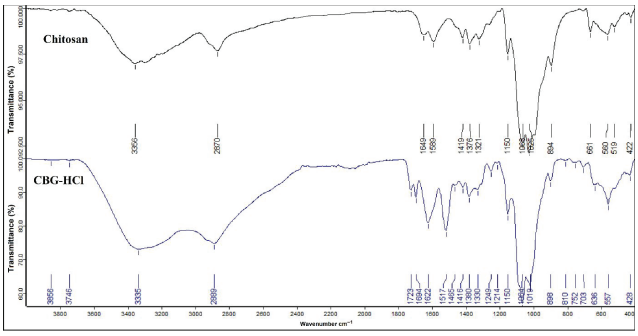

Fig. 2. FTIR chart of chitosan and chitosan biguanidine hydrochloride (CBG-HCl).

NaCl. The electrolyte was prepared using distilled water and analytical grade chemicals. All data reported in this research either current, impedance, or resistance are with respect to the geometric surface area of the working electrode. The electrochemical measurements were conducted at room temperature (25±2°C). EIS and polarization measurements were performed after attaining a steady value of the free corrosion potential by immersing the working electrode in the testing mediums for about 30 min. The polarization curves were measured potentiodynamically at scan rate 5 mV/s starting from the OCP towards the cathodic direction (ca. –250 mV vs. OCP) then the potential scan was reversed to a final potential of ca. +250 mV vs. OCP.

3. Results and discussion

3.1. EIS measurements

Electrochemical impedance spectroscopy (EIS) experiments were conducted to evaluate the corrosion inhibition efficiency of CBG-HCl and its enhancement by the synergistic effect of 0.1 M NaCl for the LCS surface in 0.5 M H_2SO_4 medium. EIS measurements were executed at OCP in a wide frequency range, from 100 kHz to 0.10 Hz, with the AC voltage amplitude of ±10 mV. The electrode was stabilized at OCP for 30 min, before the measurements. EIS data demonstrated in Figs. 3a,b present Nyquist and Bode diagrams documented during the use of low carbon steel electrode in the corrosive medium in both cases of the presence and absence of 25, 50, 70 and 100 ppm of CBG-HCl, while Figs. 3c,d present the results under the same conditions with the addition of 0.1 M NaCl. Fig. 3a shows that the diameter of the semicircle expands with the increase of inhibitor concentration in the electrolyte, and this expanding is more pronounced in Fig. 3c, with the synergistic effect of 0.1 M NaCl, indicating a growth in corrosion resistance of the LCS with the concentration increase of CBG-HCl from 25 to 100 ppm.

An electrical equivalent circuit (EEC) model shown in Fig. 4(a) was used to simulate the EIS data and define the related resistance, then computes the corresponding inhibition efficiencies. While Fig. 4 presents example of the equivalent circuit model fitting with the obtained EIS data at particular inhibitor concentrations. The equivalent circuit consists of a parallel combination of a resistor, R_p, represent-

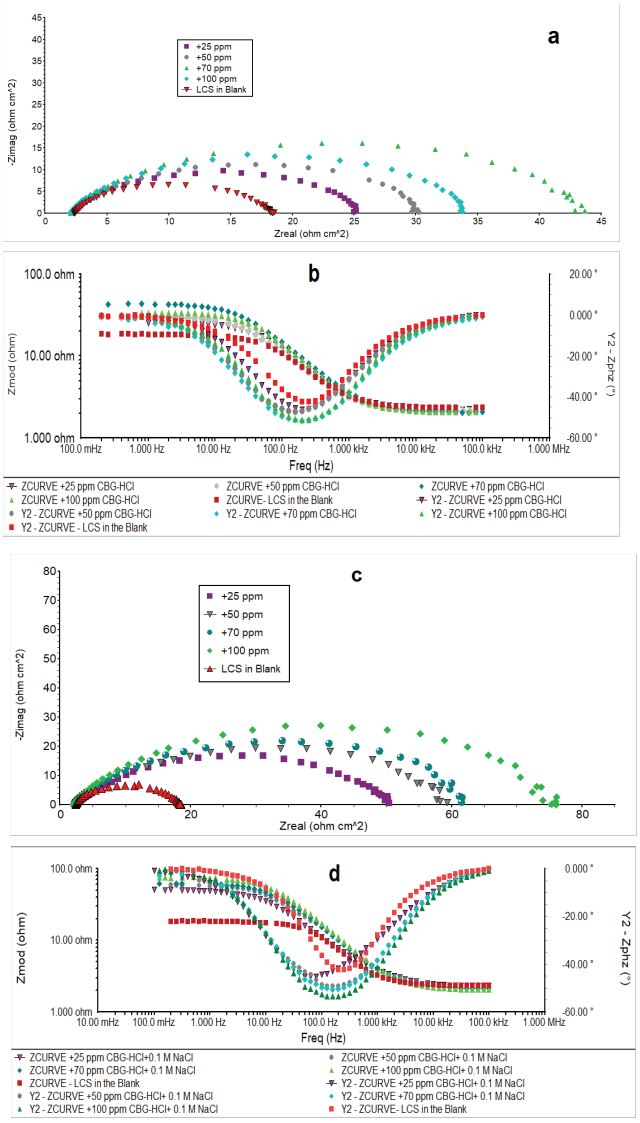

Fig. 3. (a), (b) Nyquist and Bode plots of low carbon steel obtained at different concentrations of CBG-HCl in 0.5 M H_2SO_4 at room temperature. (c) (d) Nyquist and Bode plots of low carbon steel obtained at different concentrations of CBG-HCl in 0.5 M H_2SO_4 with 0.1 M of NaCl at room temperature.

ing the polarization resistance long with a capacitor, C_{dl}, representing the double layer capacity of the electrode-electrolyte interface, in a series with the solution resistance component (R_s). The relation between the impedance of applied circuit, Z, and the frequency of the AC signal (f), R_p, R_s, and CPE_{dl}, is presented in Eq. (1) [35]:

$$Z = R_S + \left(\frac{R_P}{1 + \left(j2\pi f C_{dl} R_p \right)^{\alpha}} \right) \tag{1}$$

wherein α is an empirical parameter ($0 \le \alpha \le 1$), which indicates the extent of deviation from the ideal RC-behavior of the electrode-electrolyte interface. Due to the LCS, the surface turns rough and inhomogeneous in the sulfuric acid solution; the capacitance is presented through a constant phase element

(CPE). The related efficiencies were calculated and presented in Table 1 by using Eq. (2) [35–38]. In this EEC, R_S represents the ohmic resistance between the reference electrode and the working electrode; R_p is the polarization resistance and CPE (constant phase element) represents the capacitance of the electric double-layer at the electrode/electrolyte interface.

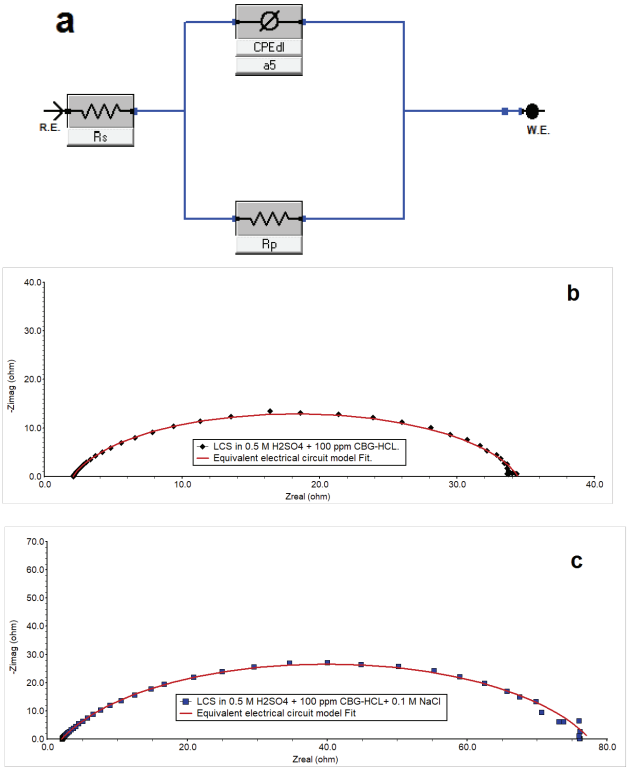

Fig. 4. (a) EEC model applied in order to simulate EIS data obtained on low carbon steel electrode immersed in the electrolyte in absence and presence of CBG-HCl inhibitor. R_s, R_p and CPE represent solution resistance, polarization resistance and the capacitance of double-layer, respectively; (b) (c) the model fitting in presence of 100 ppm CBG-HCl and inhibitor blend (100 ppm CBG-HCl + 0.1 M NaCl), respectively.

$$IE\% = \left(1 - \left[\frac{R_p^{(b)}}{R_p^{(in)}}\right] \times 100\right) \quad (2)$$

wherein $R_p^{(b)}$ and $R_p^{(in)}$ are the polarization resistances during the existence and the non-existence of the inhibitor, respectively.

Table 1 demonstrates a significant improvement in corrosion inhibition efficiency *IE* of LCS with the increasing of inhibitor concentration with the presence of 0.1 M NaCl in the electrolyte. This enhancement in *IE* is obvious in the increasing of the polarization resistance values (R_p). The highest *IE* value (79.81%) was recorded at presence of 100 ppm CBG-HCl and 0.1 M NaCl comparing to the higher *IE* of 63.71% obtained at presence of 70 ppm CBG-HCl alone.

3.2. Potentiodynamic measurements

Potentiodynamic experiments were conducted to verify the data obtained from EIS measurements. Fig. 5 illustrates potentiodynamic polarization curves recorded on a low carbon steel electrode in 0.5 M H_2SO_4 solution, in the absence and presence of 0.1 M NaCl and different concentrations of CBG-HCl. All potential measurements were conducted versus the reference electrode (saturated calomel electrode) potent ion.

From the curves in Fig. 5, in which the anodic branch represents the dissolution of LCS, while the cathodic branch represents the HER, which shifted below, it is obvious that both the anodic and cathodic current decreases with the increase of the inhibitor concentration in the solution. This proves that CBG-HCl acts a mixed-type corrosion inhibitor. The corresponding corrosion current densities (*j*) were estimated by the extrapolation of the cathodic and anodic curves to the related OCP, and presented with the calculated inhibition efficiency. Table 2 presents the results without/with the synergistic effect of 0.1 M NaCl.

Inspection of Table 2 reveals that increasing of inhibitor concentration in the electrolyte caused a pronounced inhibitive effect, against low carbon steel corrosion, by causing a marked decrease of the cathodic as well as the anodic current densities with the exist of 0.1 M NaCl, consistently with

Table 1
Present parameters of the simulated equivalent circuit and related inhibition efficiency (IE) of low carbon steel in 0.5 M H_2SO_4 containing various concentrations of CBG-HCl with and without 0.1 M NaCl

Electrolyte composition	R_p(Ω cm^2)	CPE × 10^6 (Ω^{-1} cm^{-2} Sa)	α	Goodness of fit × 10^{-6}	*IE* %
Blank (0.5 M H_2SO_4) (A)	15.25	372	0.863	87.92	–
A + 25 ppm CBG-HCl	23.37	326	0.844	123.6	34.75
A + 50 ppm CBG-HCl	28.58	252	0.869	131.0	46.64
A + 70 ppm CBG-HCl	42.02	316	0.821	146.0	63.71
A + 100 ppm CBG-HCl	32.41	260	0.857	117.8	52.93
A + 25 ppm CBG-HCl + 0.1 M NaCl	48.94	700	0.999	120.1	68.84
A + 50 ppm CBG-HCl + 0.1 M NaCl	58.04	555	0.742	975.6	73.73
A + 70 ppm CBG-HCl + 0.1 M NaCl	61.99	452	0.766	303.0	75.39
A + 100 ppm CBG-HCl + 0.1 M NaCl	75.52	391	0.782	351.5	79.81

the conclusions of Table 1. *IE* was calculated using Eq. (3) [35,36].

$$IE\% = \left(1 - \frac{j_{in}}{j_b}\right) \times 100 \quad (3)$$

where j_{in} (A cm^{-2}) is the corrosion current at a particular concentration of the inhibitor and j_b is the corrosion current in the absence of inhibitor in the bulk solution.

Fig. 6 shows the average *IE* values with standard deviation obtained using both EIS, and potentiodynamic experiments results with standard deviation conducted at 25, 50, 70 and 100 ppm concentration of CBG-HCl in the presence of 0.1 M NaCl.

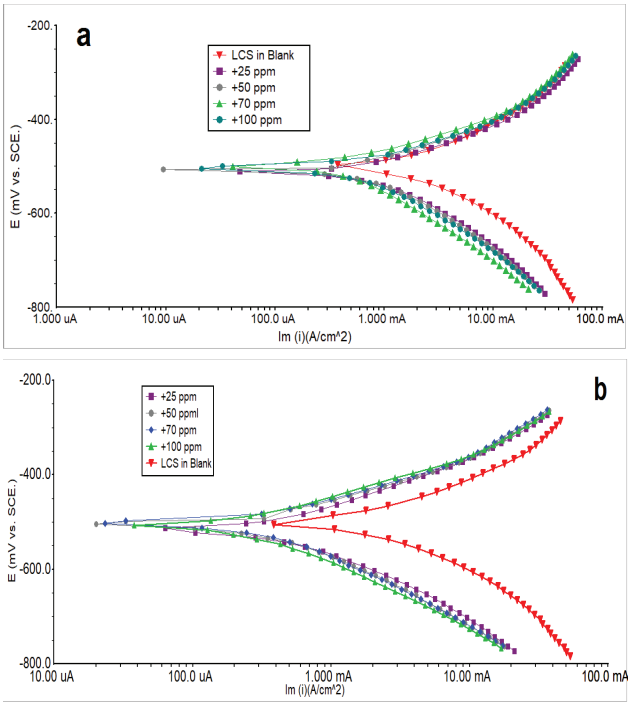

Fig. 5. (a) Potentiodynamic plots of the LCS electrode recorded at various concentrations of CBG-HCl in a 0.5 M H_2SO_4 solution. (b) Potentiodynamic plots of the LCS electrode recorded at various concentrations of CBG-HCl in a 0.5 M H_2SO_4 solution in the presence of 0.1 M NaCl. Scan rate = 5 mV/s.

3.3. Adsorption isotherm study

In order to study the adsorption of the CBG-HCl inhibitor on the LCS surface, Tempkin, Freundlish, and Langmuir adsorption isotherms were applied to the obtained inhibition data. Langmuir adsorption isotherm complied best with the data assuming that the inhibition efficiency (IE) is proportional with the inhibitor surface coverage, θ [36–40]. The mean corrosion inhibition efficiency values obtained using the two experimental techniques are used in the isotherm study and presented in Fig. 7 in the form of the linearized Langmuir isotherm by Eq. (4):

$$\frac{C}{\theta} = \frac{1}{K_{ads}} + C \quad (4)$$

where C is the inhibitor concentration, θ is the surface coverage and K_{ads} is the adsorption equilibrium constant. An inhibitor is considered to be following Langmuir if the plot of C/θ vs C is linear and the slope of the line is closed to unity. Similarly, regarding Tempkin and

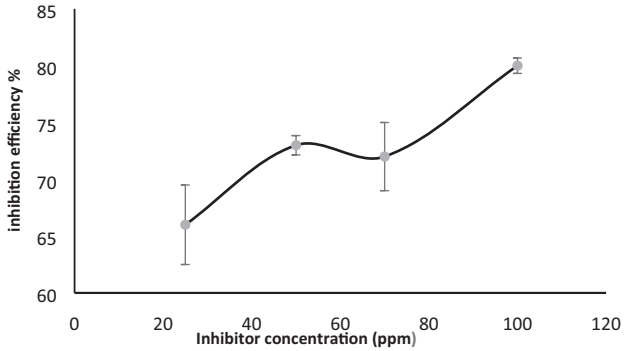

Fig. 6. The mean corrosion inhibition efficiency values of CBG-HCl on LCS at presence of 0.1 M NaCl in 0.5 M H_2SO_4 solution.

Table 2
Corrosion current density (I_{corr}), anodic and cathodic Tafel slopes (β_a and β_c, respectively), corrosion potential (E_{corr}) and *IE* recorded on low LCS in a 0.5 M H_2SO_4 solution involving various concentrations of CBG-HCl in the absence and presence of 0.1 M NaCl and the related corrosion inhibition efficiency values

Electrolyte composition	$-E_{corr}$ (mV vs SCE)	Corrosion current density (I_{corr}) (mA)	βa (mV dec^{-1})	−βc (mV dec^{-1})	*IE* (%)
Blank (0.5 M H_2SO_4) (A)	514	0.91	98	116	–
A + 25 PPM CBG-HCl	513	0.682	82	98	25.05
A + 50 PPM CBG-HCl	506	0.605	82	107	33.52
A + 70 PPM CBG-HCl	499	0.286	82	170	68.57
A + 100 PPM CBG-HCl	503	0.452	64	112	50.33
A + 25 PPM CBG-HCl + 0.1 M NaCl	518	0.337	101	91	62.97
A + 50 PPM CBG-HCl + 0.1 M NaCl	505	0.25	77	105	72.53
A + 70 PPM CBG-HCl + 0.1 M NaCl	504	0.292	90	110	67.91
A + 100 PPM CBG-HCl + 0.1 M NaCl	511	0.175	84	71	80.77

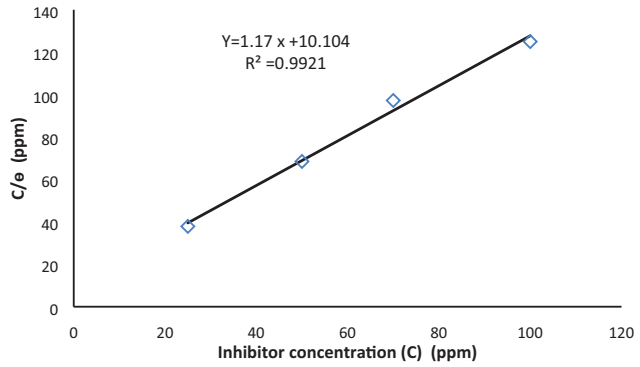

Fig. 7. Langmuir adsorption isotherm plot for the adsorption of CBG-HCl on the surface of LCS in the corrosive medium.

Table 3
Adsorption isotherms parameters carried out at room temperature

Isotherm parameters	Langmuir	Temkin	Freundlich
R^2	0.9921	0.9519	0.9596
Slope	1.1706	0.1716	0.1006

Freundlich, the plot of log θ vs log *C* should be linear. From the correlation coefficients (R^2) obtained from plots as shown in Table 3, Langmuir isotherm is better fitted into the experiment data with R^2 of 0.9921 and slope of 1.17, which is close to unity and this suggests monolayer adsorption of inhibitor on the surface of LCS. The results are best fitted to Langmuir adsorption isotherm in view of the larger value of R^2 compared to the fitting to other isotherms (as shown in Table 3). The small deviation of the slope (about 10% of unity) is within acceptable margin and might originated from the surface heterogeneity of LCS which might allow for a little contribution of multilayer and/or other adsorption modes. However, the fitting of the results with Langmuir adsorption isotherm is quite satisfactory to describe the physicochemical picture of the interface.

Adsorption equilibrium constant K_{ads} = 0.099 dm^3 mg^{-1} (L mg^{-1}) was yielded from the intercept of the line in Fig. 7, and then the corresponding standard Gibbs free energy of adsorption (kJ mol^{-1}) was calculated from Eq. (5) [36–42]:

$$K_{ads} = \frac{1}{C_{solvent}} \exp\left(\frac{-\Delta G^0_{ads}}{RT}\right) \quad (5)$$

In which *T* is the temperature (K), $C_{solvent}$ is the molar concentration of the solvent, which is water in this case, (C_{H2O} = 10^6 mg *dm*$^{-3}$) and *R* (J *mol*$^{-1}$ *K*$^{-1}$) is the gas constant. The calculated standard Gibbs free energy of adsorption of CBG-HCl on the low carbon steel surface was –28.5 kJ *mol*$^{-1}$ at 298 K. Literature shows that magnitudes of standard Gibbs free energy of adsorption in aqueous solution around or higher than (more negative) –40 kJ *mol*$^{-1}$ involve charge sharing between the molecules and the metal (chemisorption) while around –20 kJ *mol*$^{-1}$ or lower indicate adsorption with electrostatic interaction between the adsorbent and adsorbate (physisorption) [10,36,43]. Thus the corresponding calculated negative value of standard Gibbs energy of adsorption (–28.5 kJ *mol*$^{-1}$) demonstrates that the adsorption of CBG-HCl is physisorption and the negative values of $-\Delta G^0_{ads}$ ensure the spontaneity of the adsorption process and the stability of the adsorbed layer on the low carbon steel surface.

Table 4
The inhibition efficiency and corrosion resistance data recorded at selected time intervals obtained from EIS measurements conducted on low carbon steel in the presence of 100 ppm CBG-HCl and 0.1 M NaCl in a 0.5 M H_2SO_4 solution

Time	Blank solution	100 ppm CBG-HCl + 0.1 M NaCl	IE%
	$R_p^{(b)}$ (ohm cm^{-2})	$R_p^{(in)}$ (ohm cm^{-2})	
10 min	15.25	75.50	79.81
30 min	13.61	75.52	80.46
1 h	13.60	83.36	83.69
2 h	11.05	84.62	86.94
4 h	7.31	77.54	90.59
6 h	5.25	71.64	92.67

3.4. Effect of exposure time on inhibition efficiency

Electrochemical Impedes Spectroscopy (EIS) experiments were conducted in the presence of 100 ppm CBG-HCl in a 0.5 M H_2SO_4 and 0.1 M NaCl solution at selected time intervals, to determine the time needed for the inhibitor to perform the maximum inhibition efficiency and its stability at the testing conditions. The related inhibition efficiency and corrosion resistance values are presented in Table 4. The data show that even 10 min after the immersion of the working electrode in the electrolyte, the corrosion inhibition efficiency reached 79%. The maximum efficiency was reached after two hours of testing (81.98%), and remained as high as 78.71% after 6 h. The longer-lasting corrosion inhibition efficiency of CBG-HCl can also be proved by the results of weight loss experiments and by evaluating the scanning electron microscopy (SEM) results of the low carbon surface samples. Fig. 8 shows the inhibition efficiency obtained from EIS at 1 to 7 h time intervals experiments conducted on LCS in the presence of CBG-HCl (100 ppm) and 0.1 M NaCl in a 0.5 M H_2SO_4 solution.

Weight loss results showed that after 24 h of the immersion of the samples in 0.5 M H_2SO_4 in the addition and the omission of 100 ppm of CBG-HCl and 0.1 M NaCl, the IE reached 86%.

Fig. 9 shows the sample surface scan results after one day of immersion in the testing solution in the absence and presence of CBG-HCl and 0.1 M NaCl. SEM results demonstrate that in the absence of the inhibitor in the solution, the corrosion on the surface is relatively higher and it can be clearly seen that the surface is severely damaged (Fig. 9a) compared to the sample surface in Fig. 9b, which represents the less corroded surface of the sample

immersed in the corrosive solution in the presence of only CBG-HCl, while Fig. 9c shows the relatively most protected surface sample immersed in the corrosive electrolyte containing the inhibitor blend (100 ppm CBG-HCl and 0.1 M NaCl). These results prove the long-term corrosion inhibition efficiency of the blend inhibitor.

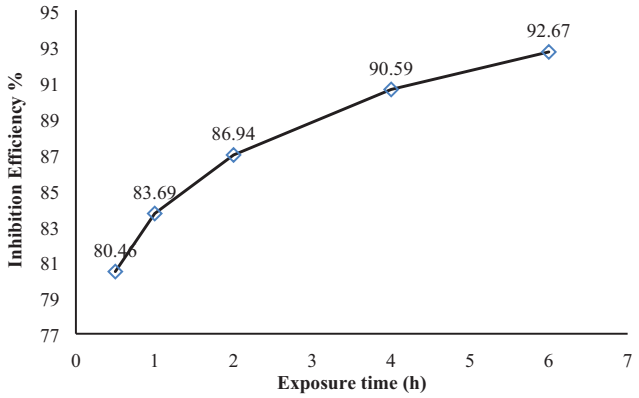

Fig. 8. The inhibition efficiency at selected time intervals obtained from EIS experiments conducted on low carbon steel after adding 100 ppm CBG-HCl and 0.1 M NaCl in a 0.5 M H_2SO_4 solution.

3.5. Corrosion inhibition mechanism and results of EDX

So far the presented results clearly illustrate that CBG-HCl is an effective inhibitor of low carbon steel corrosion in a 0.5 M H_2SO_4 solution. The plots of potentiodynamic results in Fig. 5 prove that the inhibitor performs as a mixed-type inhibitor, reducing both partial corrosion reactions. The mechanism of its inhibition action takes place by forming a surface protecting layer, which minimizes access of corrosive agents to the surface of low carbon steel by producing a tight hydrophobic barrier due to the presence of (–NH_2) group in CBG-HCl. The adsorption on the anodic sites occurs through the donor–acceptor interaction between lone pair of electrons on the NH_2 of the inhibitor molecule and Fe^{2+} ions on the surface of the metal. The quaternary amine group exists in protonated form in the acidic medium and gets adsorbed on the cathodic sites, retarding the evolution of hydrogen. Therefore, the CBG-HCl inhibits the corrosion of low carbon steel efficiently due to the presence of lone pair of electrons on nitrogen and positive charge on quaternary ammonium group.

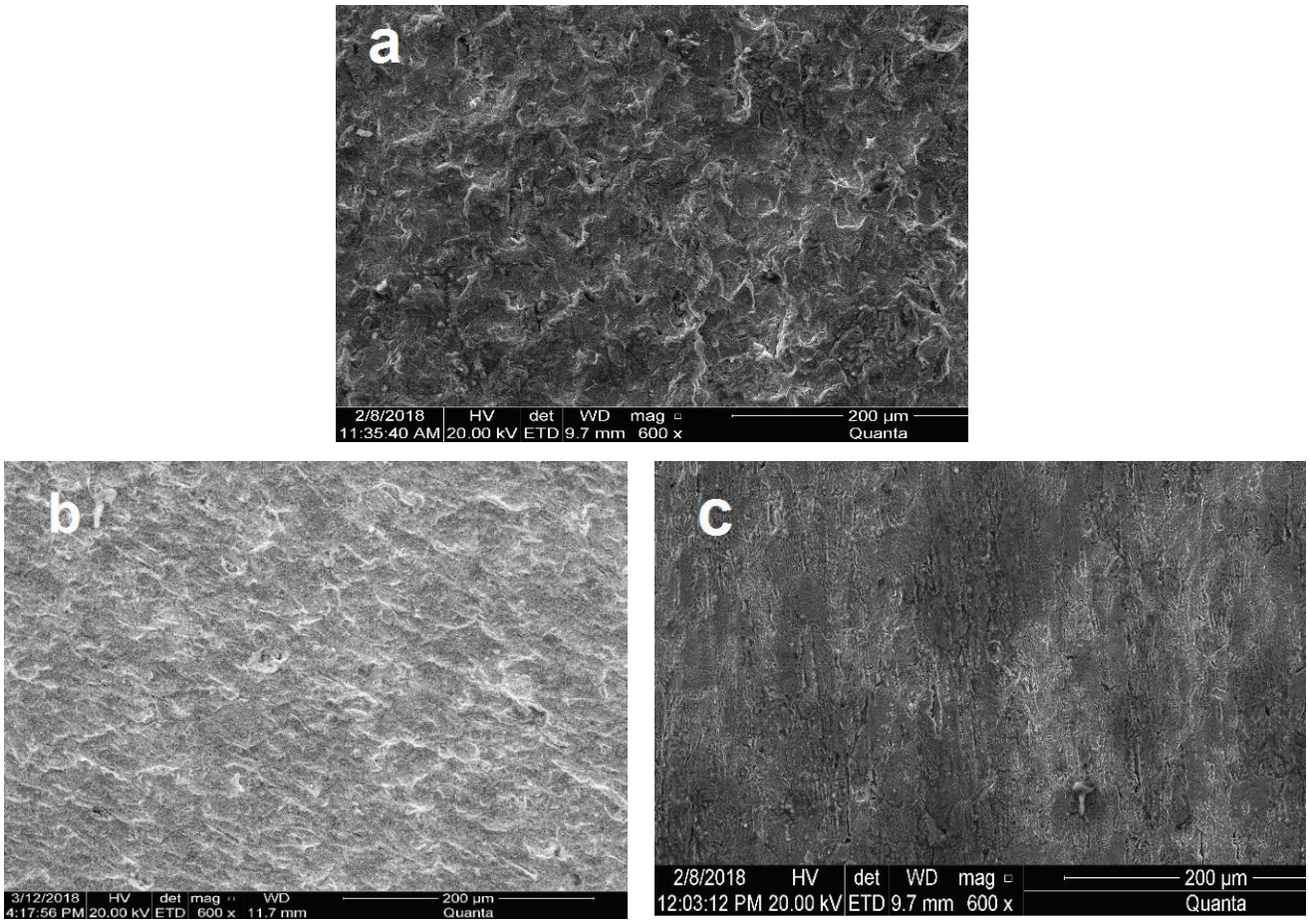

Fig. 8. The inhibition efficiency at selected time intervals obtained from EIS experiments conducted on low carbon steel after adding 100 ppm CBG-HCl and 0.1 M NaCl in a 0.5 M H_2SO_4 solution.

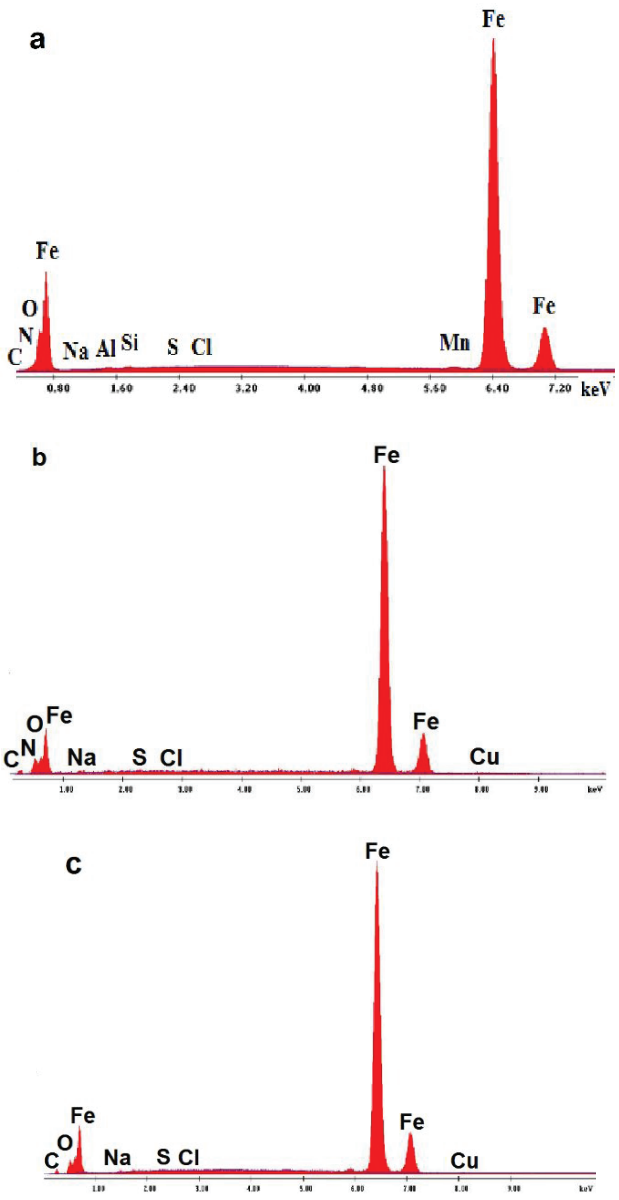

Fig. 8. The inhibition efficiency at selected time intervals obtained from EIS experiments conducted on low carbon steel after adding 100 ppm CBG-HCl and 0.1M NaCl in a 0.5M H_2SO_4 solution.

The inhibition efficiency depends on the surface coverage, then the concentration of adsorbed inhibitor molecules on the metal surface. In this regard, in order to estimate the tight of the CBG-HCl layer on the LCS surface, EDX measurements were performed. EDX results shown in Fig. 10 and Table 5 indicate a significant increase in the weight percentage of carbon, oxygen, and nitrogen elements, which are the most content of the inhibitor molecule, on the surface of LCS samples immersed for 1 h in 0.5 M H_2SO_4 solution including: (b) only100 ppm CBG-HCl, (c) blend inhibitor (CBG-HCl + 0.1 M NaCl) and (a) on fresh sample. This expansion of the element percentages on the sample of carbon steel is proportional with

Table 5
EDX results represent weight percentage of particular elements on the sample surface obtained for low carbon steel after immersion in 0.5 M H_2SO_4 in absence and presence of 100 ppm CBG-HCl and inhibitor blend (100 ppm CBG-HCl + 0.1 M NaCl) for 1 h

Element	Mass percent (wt %)		
	On fresh sample before immersion	After immersing in electrolyte contains only 100 ppm CBG-HCl	After immersing in solution contains CBG-HCl + NaCl
Carbon	1.15	2.31	3.21
Oxygen	1.66	1.95	4.81
Nitrogen	0.12	0.56	0.78

quantity of adsorbed inhibitor on the surface and with the metal surface coverage.

4. Conclusions

EIS and potentiodynamic results consistently revealed the high inhibiting efficiency (IE) of CBG-HCl and 0.1 M NaCl blend in opposition to the corrosion of low carbon steel in acidic solution. EIS and weight-loss measurements illustrated that the blend offers a satisfactory and long-lasting effective corrosion inhibition efficiency during periods of constant immersion of low carbon steel in 0.5 M H_2SO_4 solution, at low concentration of CBG-HCl (100 ppm). Potentiodynamic measurements demonstrated that CBG-HCl acts as a mixed-type inhibitor. The process of the inhibitor is accomplished through the mechanism of the inhibitor adsorption and the formation of a surface layer. This minimizes the access of the solvated corrosive agents to the LCS surface by presenting a hydrophobic barrier due to the presence of the long hydrocarbon chain. The adsorption process of the inhibitor was found to be in very good agreement with the Langmuir isotherm and it is a spontaneous monolayer adsorption and of a physisorptive type.

Acknowledgements

The authors are grateful to the Science and Technological Development Fund (STDF) of Egypt for its partial financial support of this work (Project No. CB-4874).

References

[1] S. Papavinasam, A. Doiron, T. Panneerselvam, R.W. Revie, Effect of hydrocarbon on the internal corrosion of oil and gas pipelines, Corrosion, 63 (2007) 704–712.
[2] W. Villamizar, M. Casales, J.G. Gonzalez-Rodriguez, L. Martinez, CO_2 corrosion inhibition by hydroxyethyl, aminoethyl, and amidoethyl imidazolines in water–oil mixtures, J. Solid State Electrochem., 11 (2007) 619–629.
[3] M.A. Migahed, Corrosion inhibition of steel pipelines in oil fields by *N,N*-di(polyoxy ethylene) amino propyl lauryl amide, Prog. Org. Coat., 54 (2005) 91–98.
[4] M.A. Deyab, Effect of cationic surfactant and inorganic anions on the electrochemical behavior of carbon steel in formation water, Corros. Sci., 49 (2007) 2315–2328.

[5] A. El Nemr, New Developments in Electrodeposition and Pitting Research, Research Signpost Publishers, Transworld Research Network, T.C. 37/661(2), Fort P.O., Trivandrum-695 023, Kerala, India (2007). [ISBN 978-81-7895-304-5] 445 pp.
[6] A.M. Alsabagh, M.A. Migahed, Hayam S. Awad, Reactivity of polyester aliphatic amine surfactants as corrosion inhibitors for carbon steel in formation water (deep well water), Corros. Sci., 48 (2006) 813–828.
[7] A. Asan, S. Soylu, T. Kıyak, F. Yıldırım, S.G. Oztas, N. Ancın, M. Kabasakaloglu, Investigation on some Schiff bases as corrosion inhibitors for mild steel, Corros. Sci., 48 (2006) 3933–3944.
[8] A.B. Shein, A.V. Denisova, Choice of effective corrosion inhibitors for acid treatment of wells, Prot. Met., 42 (2006) 34–42.
[9] F. Bentiss, M. Lagrenée, M. Traisnel, 2,5-Bis(n-Pyridyl)-1,3,4-Oxadiazoles as corrosion inhibitors for mild steel in acidic media, Corrosion, 56 (2000) 733–742.
[10] M. Lebrini, M. Traisnel, M. Lagrene, B. Mernari, F. Bentiss, Inhibitive properties, adsorption and a theoretical study of 3,5-bis(n-pyridyl)-4-amino-1,2,4-triazoles as corrosion inhibitors for mild steel in perchloric acid, Corros. Sci., 50 (2007) 473–479.
[11] M.S. Morad, A.M. Kamal El-Dean, 2,2-Dithiobis(3-cyano-4,6-dimethylpyridine): a new class of acid corrosion inhibitors for mild steel, Corros. Sci., 48 (2006) 3398–3412.
[12] E.S.H. El Ashry, A. El Nemr, S.A. Essawy, S. Ragab, Corrosion inhibitors Part III: Quantum chemical studies on the efficiencies of some aromatic hydrazides and Schiff bases as corrosion inhibitors of steel in acidic medium, ARKIVOC, xi, (2006) 205–220.
[13] E.S.H. El Ashry, A. El Nemr, S. Ragab, Quantitative structure activity relationships of some pyridine derivatives as corrosion inhibitors of steel in acidic medium, J. Mol. Model., 18 (2012) 1173–1188.
[14] A. El Nemr, A.A. Moneer, A. Khaled, A. El Sikaily, G.F. Elsayed, Modeling of synergistic halide additives effect on the corrosion of aluminum in basic solution containing dye, Mater. Chem. Phys., 144 (2014) 139–154.
[15] E.S.H. El Ashry, A. El Nemr, S.A. Essawy, S. Ragab, Corrosion inhibitors Part IV: Quantum chemical studies on the corrosion inhibitions of steel in acidic medium by some aniline derivatives, Chem. Phys., 1 (2006) 41–62.
[16] A. El Nemr, G. F. El Said, A. Khaled, A. El Sikaily, A.A. Moneer, D.E. Abd-El-Khalek, Differences in corrosion inhibition of water extract of *Cassia fistula* L. pods and *o*-phenanthroline on steel in acidic solutions in the presence and absence of chloride ions, Desal. Water Treat., 52 (2014) 5187–5198.
[17] G. Ji, P. Dwivedi, S. Sundaram, R. Prakash, Inhibitive effect of *chlorophytum borivilianum* root extract on mild steel corrosion in HCl and H_2SO_4 solutions, Ind. Eng. Chem. Res., 52(31) (2013) 10673–10681.
[18] C. Kamal, M.G. Sethuraman, Caulerpin—A bis-indole alkaloid as a green inhibitor for the corrosion of mild steel in 1 M HCl solution from the marine alga *caulerpa racemosa*, Ind. Eng. Chem. Res., 51 (2012) 10399–10407.
[19] S. Deng, X. Li, Inhibition by Ginkgo leaves extract of the corrosion of steel in HCl and H_2SO_4 solutions, Corros. Sci., 55 (2012) 407–415.
[20] G. Ji, S.K. Shukla, P. Dwivedi, S. Sundaram, R. Prakash, Inhibitive effect of *argemone mexicana* plant extract on acid corrosion of mild steel, Ind. Eng. Chem. Res., 50 (2011) 11954–11959.
[21] K. Alaneme, S.J. Olusegun, A.W. Alo, Corrosion inhibitory properties of elephant grass (*Pennisetum purpureum*) extract: Effect on mild steel corrosion in 1 M HCl solution, A. E. J., 55(2) (2016) 1069–1076.
[22] L. Valek, S. Martinez, Copper corrosion inhibition by Azadirachta indica leaves extract in 0.5 M sulphuric acid, Mater. Lett., 61 (2007) 148–151.
[23] M.A. Quraishi, A. Singh, V. Singh, D.K. Yadav, K.S. Ashish, Green approach to corrosion inhibition of mild steel in hydrochloric acid and sulphuric acid solutions by the extract of *Murraya koenigii* leaves, Mater. Chem. Phys., 122 (2010) 114–122.
[24] R. Rajalakshmi, S. Subashini, A. Prithiba, Acid extracts of *Ervatamia coronaria* leaves for corrosion inhibition of mild steel, Asian J. Chem., 22 (2010) 5034–5040.
[25] U.F. Ekanem, S.A. Umoren, I.I. Udousoro, A.P. Udoh, Inhibition of mild steel corrosion in HCl using pineapple leaves (*Ananas comosus* L.) extract, J. Mat. Sci., 45 (2010) 5558–5566.
[26] N.S. Patel, S. Jauhari, G.N. Mehta, Mild steel corrosion inhibition by *Bauhinia purpurea* leaves extract in 1 N sulphuric acid, Arab. J. Sci. Eng., 34 (2009) 61–68.
[27] S.A. Umoren, M.J. Banera, T. Alonso-Garcia, C.A. Gervasi, M.V. Mirífico, Inhibition of mild steel corrosion in HCl solution using chitosan, Cellulose, 20 (2013) 2529–2545.
[28] A. Jmiai, B. El Ibrahimi, A. Tara, R. Oukhrib, S. El Issami, O. Jbara, et al., Chitosan as an eco-friendly inhibitor for copper corrosion in acidic medium: protocol and characterization, Cellulose, 24 (2017) 3843–3867.
[29] M.M. Solomon, H. Gerengi, T. Kaya, E. Kaya, S.A. Umoren, Synergistic inhibition of St37 steel corrosion in 15% H_2SO_4 solution by chitosan and iodide ion additives, Cellulose, 24 (2017) 931–950.
[30] A.M. Fekry, R.R. Mohamed, Acetyl thiourea chitosan as an eco-friendly inhibitor for mild steel in sulphuric acid medium, Electrochim. Acta, 55 (2010)1933–1939.
[31] Y. Liu, C. Zou, X. Yan, R. Xiao, T. Wang, M. Li, β-Cyclodextrin modified natural chitosan as a green inhibitor for carbon steel in acid solutions, Ind. Eng. Chem. Res., 54 (2015) 5664–5672.
[32] X. Zhao, Z.-Z. Qiao, J.-X. He, Preparation of chitosan biguanidine hydrochloride and application in antimicrobial finish of wool fabric, J. Eng. Fibers Fabr., 5 (2010) 16–24.
[33] H.E. Salama, G.R. Saad, M.W. Sabaa, Synthesis, characterization, and biological activity of cross-linked chitosan biguanidine loaded with silver nanoparticles, J. Biomater. Sci. Polym. Ed., 27 (2016) 1880–1898.
[34] Y.A. Maher, M.E.A. Ali, H.E. Salama, M.W. Sabaa, Preparation, characterization and evaluation of chitosan biguanidine hydrochloride as a novel antiscalant during membrane desalination process, Arab. J. Chem., (2018).
[35] M.S. El-Deab, Interaction of cysteine and copper ions on the surface of iron: EIS, polarization and XPS study, Mater. Chem. Phys., 129 (2011) 223– 227.
[36] S. Ghareba, S. Omanovic, Interaction of 12-aminododecanoic acid with a carbon steel surface towards the development of 'green' corrosion inhibitors, Corros. Sci., 52 (2010) 2104–2113.
[37] S.A. Ali, H.A. Al-Muallem, M.T. Saeed, S.U. Rahman, Hydrophobic-tailed bicycloisoxazolidines: a comparative study of the newly synthesized compounds on the inhibition of mild steel corrosion in hydrochloric and sulfuric acid media, Corros. Sci., 50 (2007) 664–675.
[38] F. Bentiss, M. Traisnel, N. Chaibi, B. Mernari, H. Vezin, M. Lagrenee, 2,5-Bis(nmethoxyphenyl)-1,3,4-oxadiazoles used as corrosion inhibitors in acidic media: correlation between inhibition efficiency and chemical structure, Corros. Sci., 44 (2002) 2271–2289.
[39] Popova, M. Christov, A. Zwetanova, Effect of the molecular structure on the inhibitor properties of azoles on mild steel corrosion in 1 M hydrochloric acid, Corros. Sci., 49 (2007) 2131–2143.
[40] M. Lebrini, M. Lagrenee, H. Vezin, M. Traisnel, F. Bentiss, Experimental and theoretical study for corrosion inhibition of mild steel in normal hydrochloric acid solution by some new macrocyclic polyether compounds, Corros. Sci., 49 (2007) 2254–2269.
[41] M. Benabdellah, R. Souane, N. Cheriaa, R. Abidi, B. Hammouti, J. Vicens, Synthesis of calixarene derivatives and their anticorrosive effect on steel in 1 M HCl, Pig. Resin Technol., 36 (2007) 373–381.
[42] V.R. Saliyan, A.V. Adhikari, Quinolin-5-ylmethylene-3-{[8-(trifluoromethyl) quinolin-4-yl]thio} propanohydrazide as an effective inhibitor of mild steel corrosion in HCl solution, Corros. Sci., 50 (2008) 55–61.
[43] M. Ozcan, AC impedance measurement of cystine adsorption at mild steel/sulfuric acid interface as corrosion inhibitor, J. Solid State Electrochem., 12 (2008) 1653–1661.